Geophysical Research Letters

RESEARCH LETTER
10.1029/2024GL113194

Key Points:

- A special type of lightning stroke named “energetic compact stroke” (ECS) is always coincident with downward TGFs
- Three new downward TGFs were identified by the observations of ECSs
- More than 60% of downward TGFs in winter thunderstorms in Japan are associated with ECSs

Supporting Information:

Supporting Information may be found in the online version of this article.

Correspondence to:
T. Wu,
wu.ting.x4@f.gifu-u.ac.jp

Citation:
Wu, T., Smith, D. M., Wada, Y., Nakazawa, K., Oguchi, M., Kamogawa, M., et al. (2025). Energetic compact strokes as the major source of downward terrestrial gamma-ray flashes in winter thunderstorms. *Geophysical Research Letters*, *52*, e2024GL113194. https://doi.org/10.1029/2024GL113194

Received 19 OCT 2024
Accepted 16 FEB 2025

Energetic Compact Strokes as the Major Source of Downward Terrestrial Gamma-Ray Flashes in Winter Thunderstorms

Ting Wu[1], David M. Smith[2], Yuuki Wada[3], Kazuhiro Nakazawa[4,5], Manari Oguchi[5], Masashi Kamogawa[6], Tomoyuki Suzuki[6], Qingliu Yang[1], and Daohong Wang[1]

[1]Department of Electrical, Electronic and Computer Engineering, Gifu University, Gifu, Japan, [2]Physics Department, Santa Cruz Institute for Particle Physics, University of California, Santa Cruz, CA, USA, [3]Division of Electrical, Electronic and Information Engineering, Graduate School of Engineering, Osaka University, Suita, Japan, [4]Kobayashi-Maskawa Institute for the Origin of Particles and the Universe, Nagoya University, Nagoya, Japan, [5]Graduate School of Science, Nagoya University, Nagoya, Japan, [6]Natural Disaster Research Section, Global Center for Asian and Regional Research, University of Shizuoka, Shizuoka, Japan

Abstract Terrestrial gamma-ray flashes (TGFs) are short bursts of intense gamma radiation associated with lightning discharges. Although thousands of TGFs have been observed from space, TGFs detected at ground level, known as downward TGFs, are still very limited, and their relationship with lightning discharge processes remains elusive. Here we report a special type of strong negative lightning stroke, termed energetic compact stroke (ECS), in winter thunderstorms in Japan, and provide strong evidence that ECSs are consistently associated with downward TGFs. Based on this relationship, we successfully identified three new downward TGFs by the observations of ECSs. Further, 12 out of 19 (63%) of downward TGFs analyzed in this paper were associated with ECSs, indicating that ECSs are the major source of downward TGFs in winter thunderstorms in Japan. These findings open up the possibility of remotely monitoring a large fraction of downward TGFs with simple lightning observations.

Plain Language Summary Terrestrial gamma-ray flashes (TGFs) are the most intense natural sources of gamma-ray emissions on Earth. It is well established that TGFs are coincident with lightning discharges, but it is still largely unclear what lightning discharge processes can produce TGFs and under what circumstances. In this paper, we provide strong evidence that a special type of negative lightning stroke, referred to as “energetic compact stroke” (ECS), in winter thunderstorms is consistently associated with downward TGFs. This finding makes it possible for future studies to investigate TGF mechanisms by simply observing ECSs. We also found that a large portion, 63% in this study, of downward TGFs were associated with ECSs. This unexpectedly high percentage opens up the possibility of remotely monitoring downward TGFs over wide areas simply through the detection of lightning.

1. Introduction

Terrestrial gamma-ray flashes (TGFs) are short bursts of intense gamma-ray emissions emanating from thunderstorms, with energies reaching up to 40 MeV (Marisaldi et al., 2010), making them one of the most energetic natural photon-emitting phenomena on Earth. A key question in the investigation of TGFs in recent years is their connection to lightning discharge processes. Coordinated with ground-based observations, it is well established that TGFs observed from space are often associated with initial upward negative leaders in intracloud flashes (Cummer et al., 2005, 2015; Lu et al., 2010; Shao et al., 2010; Stanley et al., 2006). However, it has also been clear that TGFs are only produced in less than 1% of lightning flashes (Albrechtsen et al., 2019; Smith et al., 2011, 2016). Although a special type of intracloud lightning discharge, known as “energetic incloud pulse” (EIP) (Lyu et al., 2015), has been reported to be consistently associated with TGFs (Lyu et al., 2016, 2021), EIPs only represent a very small fraction of lightning discharges. As a result, the production of TGFs remains highly unpredictable, and their connection with lightning discharges is still unclear.

TGFs have also been observed by ground-based instruments. They are called downward TGFs and share similar characteristics with upward TGFs observed from the space (Belz et al., 2020; Dwyer et al., 2004, 2012; Hare et al., 2016; Ortberg et al., 2024; Smith et al., 2018; Tran et al., 2015; Wada et al., 2020, 2022). Ground-based observations offer the advantage of more detailed and targeted studies of TGFs. However, because gamma rays are rapidly attenuated by the atmosphere at low altitudes, downward TGFs can only be observed at very short distances (a few kilometers at most). To date, only a handful of downward TGFs have been observed in summer (R. U. Abbasi et al., 2018; Belz et al., 2020; Dwyer et al., 2004, 2012; Hare et al., 2016; Tran et al., 2015), and the results are inconclusive, making the prospect of establishing a consistent relationship between TGFs and lightning discharges more uncertain.

Fortunately, observations in winter thunderstorms have yielded promising results. Due to their low altitudes, winter thunderstorms provide a unique condition for studying downward TGFs and their relationship with lightning discharges. Interestingly, it has been found that downward TGFs are often associated with lightning discharges producing a special type of strong low-frequency (LF) pulses (Hisadomi et al., 2021; Wada et al., 2020). Initially these strong pulses were hypothesized to be caused by upward lightning (Ishii & Saito, 2009) or EIPs (Wada et al., 2020), but they were later confirmed to be strong negative cloud-to-ground (CG) strokes (Wu, Wang, Huang, & Takagi, 2021). In this paper, we refer to these strong strokes as "energetic compact strokes" (ECSs). Further coordinated observations of TGFs and lightning discharges suggest that TGFs associated with ECSs may be common in winter thunderstorms in Japan (Ortberg et al., 2024; Wada et al., 2022). This naturally raises the question: are ECSs always coincident with TGFs, and what proportion of downward TGFs in winter thunderstorms in Japan are associated with ECSs?

In this paper, by analyzing downward TGFs observed by three different groups over multiple winter seasons, we will provide strong evidence that ECSs are consistently associated with downward TGFs. Additionally, we will demonstrate that a significant proportion, larger than 60% based on the data of current study, of downward TGFs are associated with ECSs. These findings will significantly facilitate future observations of downward TGFs.

2. Observations

2.1. TGF Observations and Identification

Multiple ground-based detectors operated by different groups are used in this study to provide the timing information of TGFs. Locations of these detectors are shown as black diamonds in Figure 1 and also in Figure S1 in Supporting Information S1.

TGF observations at A in Figure 1 are operated by a collaboration of the University of California, Santa Cruz and Shizuoka University, including two instruments: GODOT (Gamma-ray Observations During Overhead Thunderstorms) and THOR (Terrestrial High-Energy Observations of Radiation) (Ortberg et al., 2024). The GODOT consists of three scintillators, all of which are cylinders with equal length and diameter: two BC-408 plastic scintillators with 2.5 and 12.5 cm, respectively, in each dimension, and a sodium iodide (NaI) scintillator with 12.5 cm in each dimension (Bowers et al., 2017). The GODOT has a timing accuracy of 1 ms. The THOR started operation in November 2021 and provides a high timing accuracy of better than 1 μs. It consists of three plastic scintillators, one rectangular prism of $2.5 \times 2.5 \times 1.0\ cm^3$, one cylinder of diameter 7.6 cm and length 5.7 cm, and a large rectangular prism of $11.4 \times 15.2 \times 21.6\ cm^3$, plus a NaI detector of diameter 5.1 cm and length 12.7 cm.

TGF observations at B in Figure 1 are operated by the group from Osaka University. The instrument consists of one $1 \times 1 \times 1\ cm^3$ plastic scintillator for low-sensitivity observation and one $5 \times 5 \times 5\ cm^3$ plastic scintillator for high-sensitivity observation. The timing accuracy is better than 1 μs. It should be noted that the detector at B uses the signal from a low-sensitivity very-high-frequency (VHF) antenna at the same location as the triggering source. The TGF data at B are only available after November 2020.

TGF observations at C, including five different sites, are operated by a collaboration of Nagoya University and Osaka University. At each site, there is at least one $25 \times 8 \times 2.5\ cm^3$ $Bi_4Ge_3O_{12}$ (BGO) scintillator (Wada et al., 2022). All instruments at C have a timing accuracy of better than 1 μs, and the data are only available after November 2022.

Downward TGFs are identified by their characteristic gamma-ray signals, one example shown in Figure 2. Figures 2b and 2d show LF waveforms of an ECS, and Figures 2a and 2c show the corresponding gamma-ray signals, with time zero aligned with the peak of the ECS pulse. The gamma-ray signals associated with the ECS started with one large pulse near the saturation level (5 V), followed by a large undershoot lasting a few

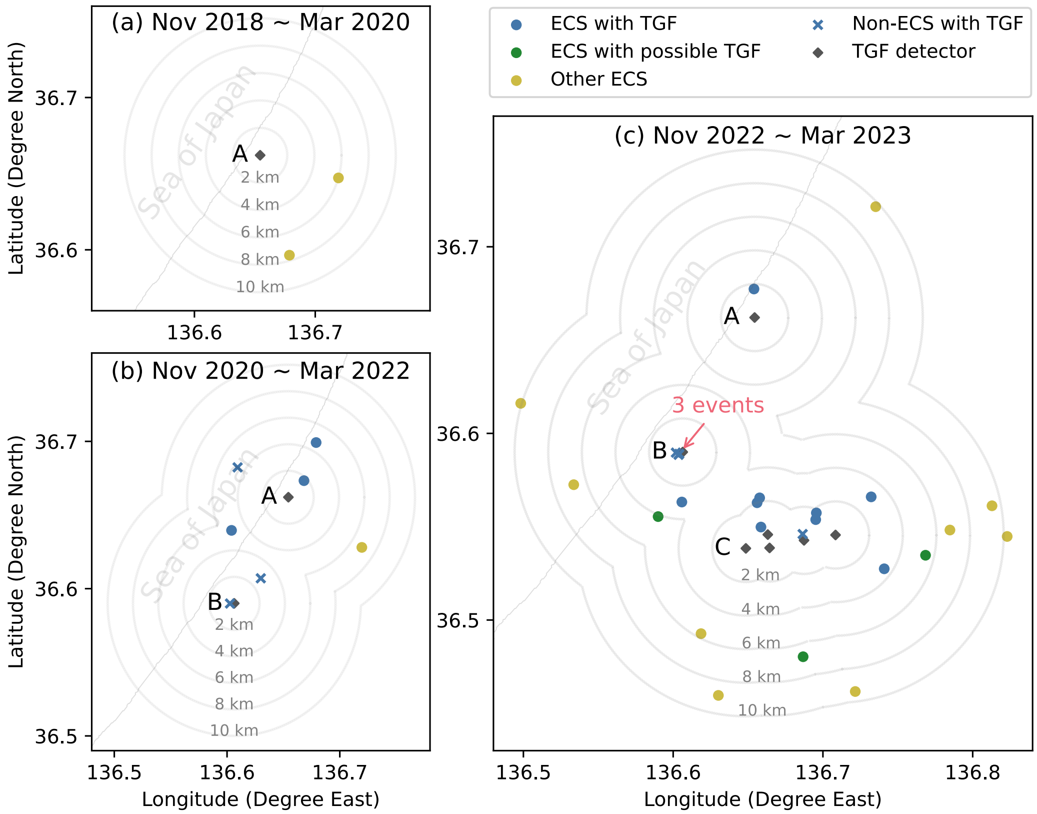

Figure 1. Locations of TGF detectors and ECSs in different observation seasons. Blue dots represent ECSs coincident with TGFs recorded by at least one detector. Green dots represent ECSs coincident with weak gamma-ray signals that are possibly TGFs. Yellow dots represent ECSs without coincident observations of TGFs. Blue crosses represent non-ECS lightning discharges coincident with TGFs. Black diamonds represent TGF detectors. A, B, and C indicate TGF detectors operated by different groups.

milliseconds. These are signatures of intense and short gamma radiations characteristic of TGFs (Hisadomi et al., 2021; Wada et al., 2019, 2022) and are distinctively different from gamma radiation of cosmic rays or radioactive materials in the environment. The first large pulse is treated as the onset of the TGF, indicated by the yellow line in Figure 2c. Note that the spacing between data points in Figures 2a and 2c is due to the saturation of detectors by TGF photons, and because of the saturation, we can only determine the onset of TGFs but not other properties such as their durations.

2.2. Lightning Observations

Lightning discharges are observed by an LF lightning mapping system called "fast antenna lightning mapping array" (FALMA) (Wu et al., 2018, 2020). FALMA typically consists of more than 10 observation sites separated by tens of kilometers. At each site, there is a flat plate antenna working in the frequency band from about 500 Hz to 500 kHz, recording electric field change waveforms from lightning discharges. Based on the arrival times of signals at different sites, FALMA is capable of determining accurate time and location of lightning discharges. Locations of FALMA sites are shown as blue squares in Figure S1 in Supporting Information S1.

Electric field change waveforms, simply referred to as LF waveforms, are used to identify different types of lightning discharges and to estimate peak currents. Procedures of peak current estimations for FALMA are described by Wu, Wang, and Takagi (2021). FALMA waveform data have been used in many studies to identify lightning discharges associated with TGFs and related high energy phenomena (Ortberg et al., 2024; Tsurumi et al., 2023; Wada et al., 2023). The atmospheric electricity sign convention is used in this paper, so a negative return stroke produces an initial positive electric field change.

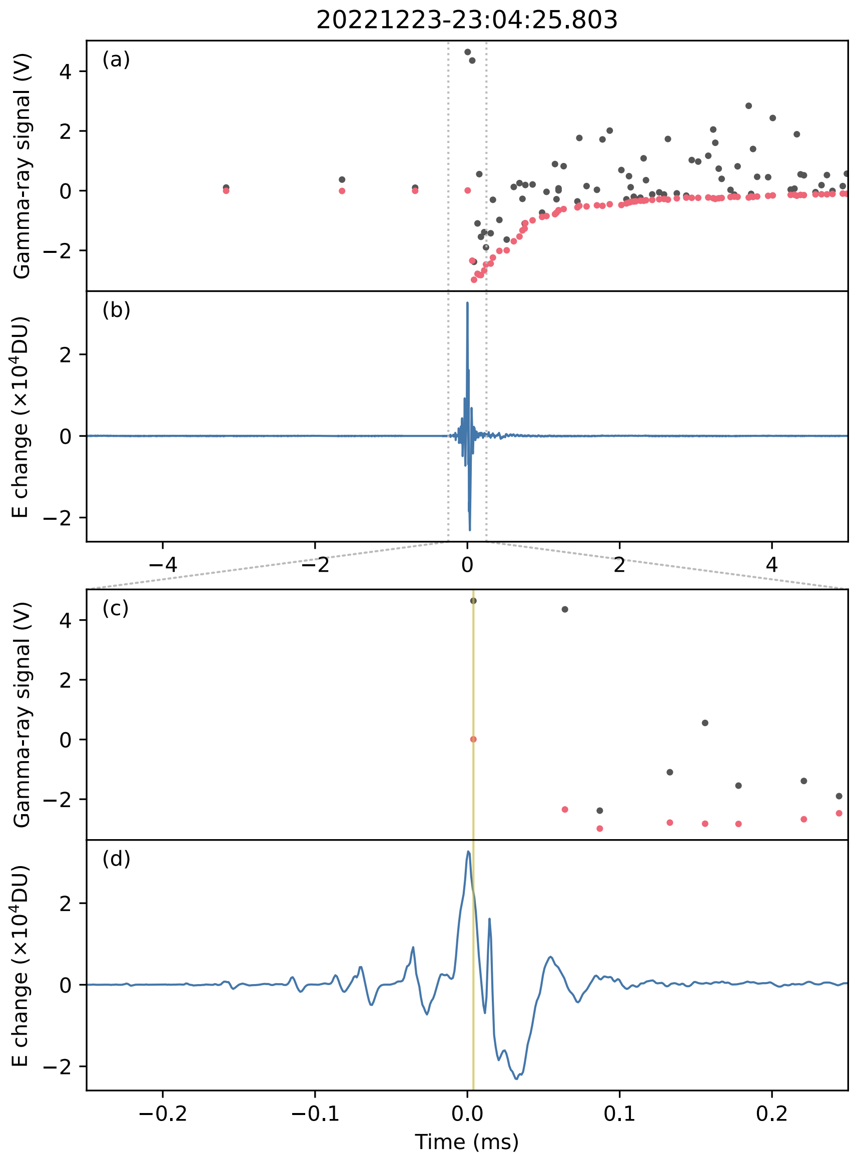

Figure 2. Gamma-ray signals associated with an ECS. (a) and (c) Gamma-ray signals. Black dots represent the pulse height and red ones the waveform baseline. (b) and (d) LF waveforms of the ECS. Time zero corresponds to the peak of the ECS pulse. The yellow line indicates the onset of the TGF.

3. Results

3.1. ECSs Coincident With TGFs

Based on the timing information of TGFs recorded by all the TGF detectors in Figure 1, we examined lightning waveforms recorded by the FALMA that are coincident with these TGFs, and identified a total of 12 ECSs over five winter seasons, from November 2018 to March 2023. For 10 of these events, we have precise timing information for the TGFs, and LF waveforms of these 10 ECSs are shown in Figures 3a–3j. The ECS in Figure 3g has also been shown in Figure 2. Waveforms of the remaining two ECSs are shown in Figure S2 in Supporting Information S1.

As can be seen in Figure 3, waveform characteristics of these ECSs are strikingly similar, featuring a large pulse preceded by smaller pulses with typical duration of a few hundred microseconds. It is now clear that the large pulse is produced by a negative return stroke and the preceding small pulses are produced by a downward negative leader (Wu, Wang, Huang, & Takagi, 2021), so ECSs are essentially negative CG strokes. However, the

10.1029/2024GL113194

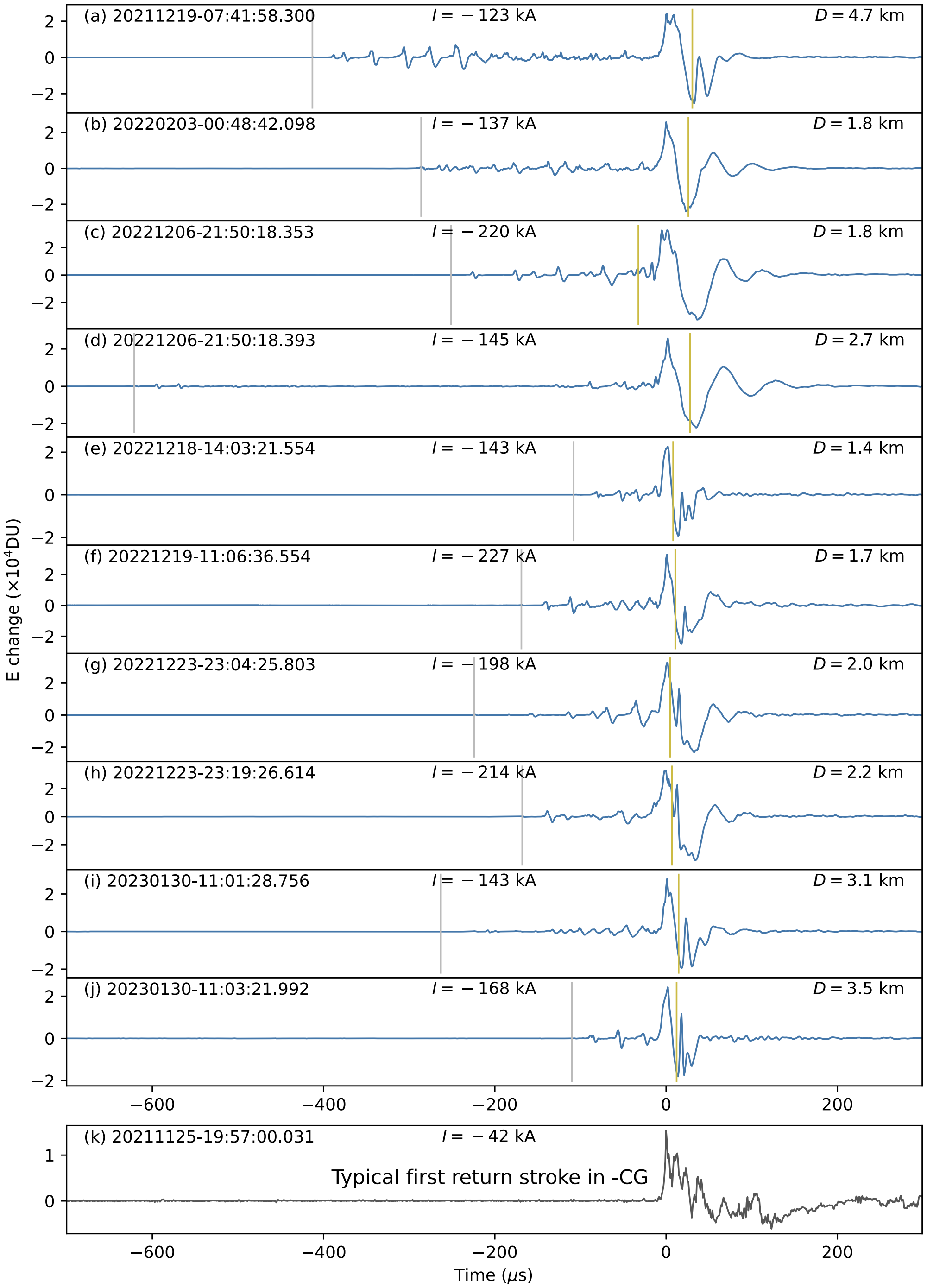

Figure 3. (a–j) LF waveforms of ECSs coincident with TGFs. Vertical gray lines represent the first leader pulse (the start of the lightning flash). Yellow vertical lines represent the onset of TGFs. The propagation time is corrected by considering horizontal distances between ECSs and corresponding detectors. Values of I represent estimated peak currents of ECSs. Values of D represent distances from the ECS to the detector detecting the TGF. (k) Waveform of a typical first return stroke in a negative CG flash.

waveforms of ECSs exhibit systematic differences from those of normal CG strokes. The following distinctive characteristics can be seen from Figure 3. For comparison, the waveform of a typical negative first return stroke is shown in Figure 3k, which is also shown in Figure S3 in Supporting Information S1 for more details.

1. Leader duration is extremely short. In Figure 3, gray lines indicate the first leader pulse (the start of each lightning flash) in each event. We can see in most cases, the leader durations of ECSs are shorter than 0.5 ms.
2. There are usually no apparent two stages of preliminary breakdown (PB) and stepped leaders before the return stroke. Normally, a CG stroke starts with PB pulses, followed by smaller stepped leader pulses, leading up to the first return stroke (Shi et al., 2019). However, in most ECSs, pulses preceding the return stroke cannot be divided into two different stages as PB and stepped leader.
3. Leader pulses are relatively strong. Stepped leader pulses right before return strokes in normal CG strokes are usually so weak that they are barely noticeable when plotted alongside return strokes. But in most ECSs, leader pulses are readily recognizable.
4. Return stroke pulses of ECSs are different from regular return stroke waveforms such as the one in Figure 3k in several respects. They are usually bipolar pulses with similar rise time and fall time and similar amplitudes of positive and negative cycles. Their pulse widths are usually small compared with regular return strokes, and they do not have the fine structures superimposed on the falling part.
5. A small pulse is often observed during the negative cycle of return stroke pulses in ECSs (Figures 3a, 3e–3j). This pulse has been inferred to be the "reflection pulse" generated when the return stroke wave is reflected from the upper end of the return stroke channel (Wu, Wang, Huang, & Takagi, 2021). Recent observations by Jensen et al. (2024) with a broadband interferometer also suggested that it may be produced by the TGF itself. Such reflection pulse would appear very peculiar for a regular return stroke waveform, and we suggest that it can be treated as a distinguishing feature of ECSs.

Figure 3 also shows the timing of TGF onset relative to the ECS waveform. Notice that the propagation time is corrected by considering the horizontal distances between ECSs and corresponding detectors. In most events, the start time of TGF corresponds to the time after the positive peak but before the negative peak of the return stroke pulse of ECSs. Interestingly, when a reflection pulse is present, as seen in events in Figures 3a, 3e–3j, the TGF always starts before the reflection pulse. There is only one event (Figure 3c) in which the TGF started before the return stroke. These results are in agreement with previous observations of TGFs associated with ECSs (Ortberg et al., 2024; Wada et al., 2020, 2022). It is also worth noting that the event in Figure 3c is also unusual as it is followed closely by the event in Figure 3d with a time difference of only about 40 ms and a horizontal distance of 3.4 km. There are no lightning signals between these two ECSs so they are treated as two separate events (see Figure S4 in Supporting Information S1).

3.2. The Possibility That ECSs Are Always Associated With TGFs

In order to investigate if ECSs are always associated with TGFs, we searched ECSs within a 10 km radius of any detector in Figure 1. According to the waveform characteristics described in Section 3.1, we identified ECSs from LF waveforms recorded by FALMA with the following two simple criteria. We also manually checked all identified waveforms and confirmed that they have the same characteristics as those in Figure 3.

1. The pulse has a negative peak current with an absolute value larger than 100 kA.
2. The pulse is preceded by weaker negative pulses with total duration shorter than 1 ms.

The identified ECSs are represented by colored dots in Figure 1. Blue dots represent ECSs coincident with TGFs. LF waveforms of these ECSs have been shown in Figure 3 (two of the events lacking accurate TGF timing information are shown in Figure S2 in Supporting Information S1). As seen in Figure 1, ECSs within 4 km of the nearest detector are all coincident with TGFs. Two ECSs with distances larger than 4 km, one 5.1 km and the other 4.7 km, in Figure 1b, are also coincident with TGFs. Ortberg et al. (2024) made a detailed analysis of these two events about possible reasons why TGFs could be observed at such large distances by ground-based detectors.

On the other hand, yellow dots in Figure 1 represent ECSs without coincident observations of TGFs. They are mostly located more than 6 km from the nearest detector (the shortest distance is 5.7 km). It is likely that these ECSs were also accompanied by TGFs, but the large distances made these TGFs undetectable. LF waveforms of these ECSs are shown in Figure S5 in Supporting Information S1, and it is clear that they have similar features as those of ECSs coincident with TGFs shown in Figure 3.

For three events represented by green dots in Figure 1c, their LF waveforms are shown in Figures 4a–4c, and it is clear that they are typical ECSs, similar to those in Figure 3. There were no definitive signals indicative of TGF occurrences so they were not immediately recognized as downward TGFs. However, the confirmation of ECSs

10.1029/2024GL113194

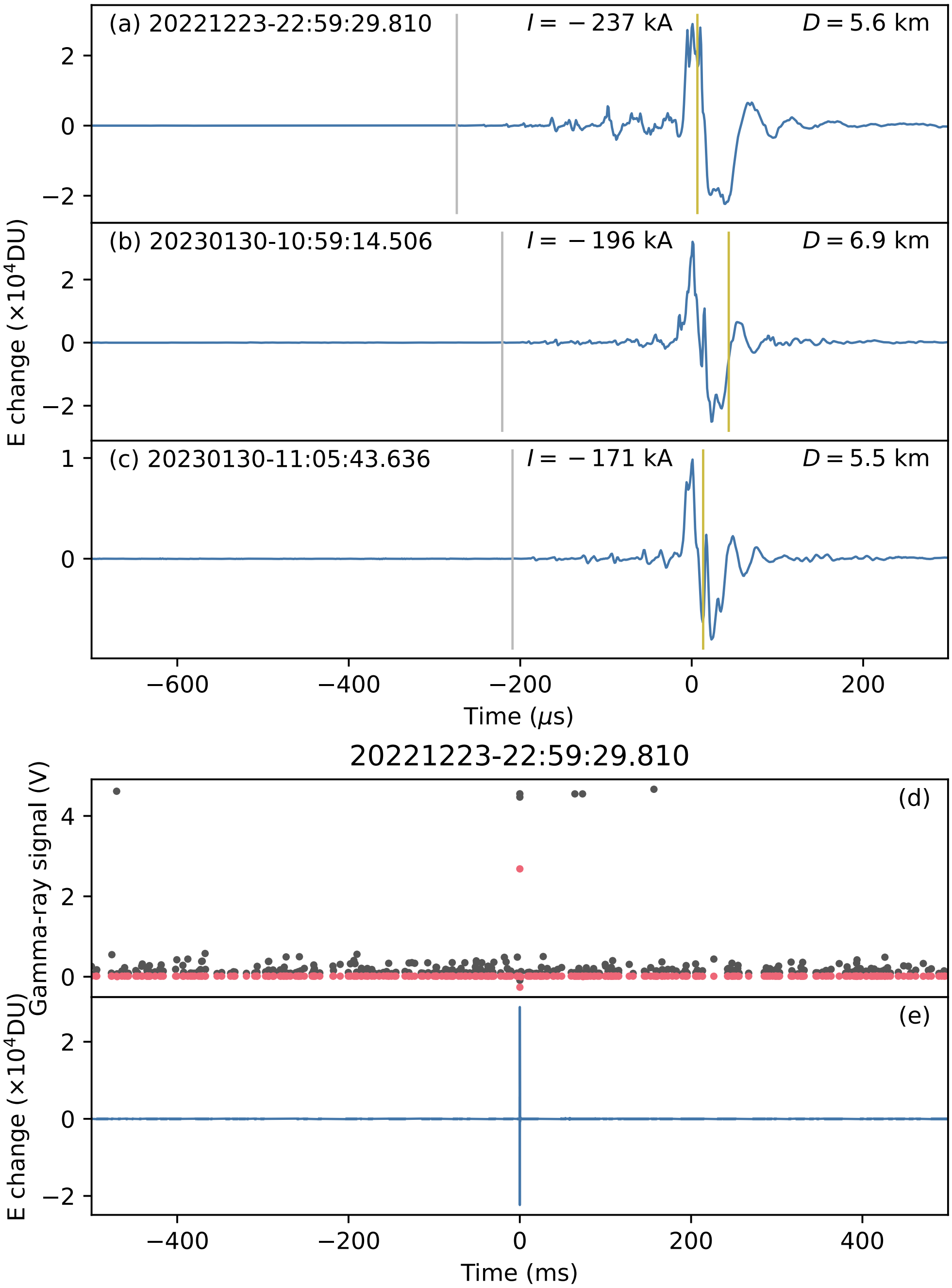

Figure 4. (a)–(c) The same as Figure 3 but for waveforms of ECSs coincident with weak gamma-ray signals. (d) and (e) Gamma-ray signals and LF waveform of the ECS in (a) shown on a time scale of 1 s.

prompted us to reexamine the gamma-ray signals and we found one gamma-ray pulse in each event, indicated by the yellow lines in Figures 4a–4c, that coincided precisely with the ECS pulses. As an example, the gamma-ray signals associated with the ECS in Figure 4a are shown in Figure 4d along with its LF waveform on a time scale of 1 s. In Figure 4d, although there are a few large pulses close to the saturation level, with one pulse also having a small undershoot, they lack the large undershoot as shown in the example in Figure 2. Such gamma-ray signals could also be produced by cosmic rays. Therefore, from the gamma-ray signals alone, this event could not be recognized as a downward TGF.

However, based on the correspondence of the gamma-ray signals with the ECS, we can estimate that the likelihood of cosmic-ray origin is extremely low, similar to the estimation by R. Abbasi et al. (2017). During the 1-s period around the ECS, there are a total of six large gamma-ray pulses represented as black dots above the 4-V level in Figure 4d. One of these large pulses aligns precisely with the ECS pulse. Denoting the number of large gamma-ray pulses as $N = 6$ within the time interval $T = 1$ s, and considering the ECS pulse duration as $\Delta t = 100$ μs, we can estimate the possibility that the large gamma-ray pulse coincidentally aligned with the ECS pulse but was actually produced by cosmic rays as

$$1 - \left(\frac{T - \Delta t}{T}\right)^N \approx 0.06\% \quad (1)$$

The actual duration of ECS pulses is shorter than 100 μs, so the possibility is even lower than 0.06%. This result suggests that when a large gamma-ray pulse corresponds right to an ECS pulse, it almost undoubtedly indicates the occurrence of a downward TGF, even though the gamma-ray signal is indistinguishable from those produced by cosmic rays.

The above results provide strong evidence that ECSs are consistently associated with TGFs, which can be detected as long as the nearest detector is within approximately 4 km. They also demonstrate the effectiveness of using ECSs as a proxy for identifying downward TGFs.

3.3. Percentage of TGFs Associated With ECSs

In addition to ECSs, TGFs in winter thunderstorms have also been observed to be associated with weaker lightning discharges (Wada et al., 2022). In Figure 1, blue crosses represent these non-ECS lightning discharges linked to TGFs. There are seven such events in the analyzed observation seasons, compared to 12 ECSs associated with TGFs represented by blue dots in Figure 1 (three newly identified events represented by green dots are not included). In other words, during the analyzed observation periods, 63% of TGFs were associated with ECSs.

It is also worthwhile to calculate the percentage separately for detectors at A, B, and C in Figure 1, as they are operated by different groups and use different instruments. For the detector at A, during five winter seasons, it recorded five TGFs, four of which were associated with ECSs. For detectors at C, during one winter season, they recorded eight TGFs including seven associated with ECSs. Therefore, the percentages for detectors at A and C are 80% and 88%, respectively. However, for the detector at B, during three winter seasons, it recorded six TGFs but only one was associated with an ECS, so the percentage is only 17%.

There are two main reasons for the exceptionally low percentage for the detector at B. First, as described in Section 2.1, the detector at B was not triggered by gamma-ray signals but by lightning signals via a low-sensitivity VHF antenna, and it seems that the VHF system even cannot be triggered by some nearby ECSs. This is evident in Figure 1c, where one ECS represented as a green dot occurred about 4 km from the detector at B, but no signal was recorded. In contrast, a detector at C with a distance of 5.6 km recorded weak gamma-ray signals from this ECS (Figure 4a). Similarly, in Figure 1b, one ECS (blue dot) has almost equal distances from detectors at A and B. While the detector at A recorded a TGF, the detector at B did not record any signal. These observations suggest that the detector at B is less likely than other detectors to detect TGFs associated with ECSs. Second, the area around B appears to have a high density of TGFs with non-ECSs. Notably, Figure 1c shows three non-ECS TGFs clustered near the same location (labeled as "3 events"), and Figure 1b shows another event at the same spot. The reason is that there is a communication tower here, and it is likely that the presence of the tower increases the frequency of lightning discharges as well as TGFs, but these tower-associated lightning discharges are rarely ECSs.

Therefore, considering the above factors responsible for the exceptionally low percentage for the detector at B, it is possible that the actual overall percentage of downward TGFs associated with ECSs is much higher than the current result of 63%, indicating that ECSs are the major source of downward TGFs in winter thunderstorms in Japan.

4. Discussion

In this paper, we provided strong evidence that ECSs are consistently associated with downward TGFs, a relationship previously only observed in a strong type of in-cloud discharge known as EIPs (Lyu et al., 2015). However, EIPs are relatively rare; so far only a handful of EIP-TGF pairs have been reported (Lyu et al., 2021). By contrast, our study alone provides 15 confirmed ECS-TGF pairs, including three newly identified from LF waveforms of ECSs. Although EIP and ECS waveforms share certain similarities, such as large amplitudes, we believe they are fundamentally different phenomena. As observed by Tilles et al. (2020) with a broadband lightning interferometer, EIP waveforms are likely generated by relativistic electron acceleration (Dwyer, 2012; Liu & Dwyer, 2013) rather than conventional lightning discharges. In contrary, ECS waveforms are unequivocally produced by negative return strokes (Wu, Wang, Huang, & Takagi, 2021), where their large amplitudes are the direct result of large return stroke currents.

In addition to their large return stroke currents, ECSs are also characterized by the large speed of preceding downward negative leaders (Wu, Wang, Huang, & Takagi, 2021), both of which indicate the presence of a strong background electric field. Notably, previous observations of TGFs occurring after negative return strokes also showed that the return strokes had large peak currents (Dwyer et al., 2012; Tran et al., 2015). Furthermore, the finding that most TGFs initiate right before the "reflection pulses," as illustrated in Figure 3, suggests that TGFs are likely produced when the return stroke wave reaches the channel top, forming a strong electric field with the negative charge region in thunderclouds. The short channels of ECSs further ensure that the return stroke current remains relatively unattenuated upon reaching the channel top. These features collectively create highly favorable conditions for TGF productions in association with ECSs and also suggest that the source of these TGFs is likely at the top of the return stroke channel.

Our results also show that 63% of the downward TGFs analyzed in this study, and probably an even larger fraction of all downward TGFs in winter, are associated with ECSs. This finding implies that the spatial distribution of downward TGFs is likely very similar to that of ECSs. Therefore, it has become very easy to investigate the spatial and temporal distributions of a major fraction of downward TGFs in a wide area by simply observing ECSs. The spatial and temporal distributions will be especially useful for identifying key factors responsible for the production of downward TGFs. These analyses will be carried out in our following studies. It is also worthwhile to note that ECSs are not unique to winter thunderstorms in Japan (Jensen et al., 2024), so an investigation of the global distribution of ECSs will also provide valuable results.

Finally, we point out that the criteria used in this paper to identify ECSs are only tentative; it is entirely possible that some negative strokes with waveform features similar to those of ECSs in Figure 3, but with peak currents weaker than 100 kA, are also associated with downward TGFs. It would be particularly interesting to find out if the relatively weak "compact strokes" reported by Wu, Wang, and Takagi (2021), previously known as "large bipolar events" (Wu et al., 2014), are linked to downward TGFs. Weak compact strokes may be essentially the same as ECSs, but they mostly occur in mountainous regions (Wu, Wang, & Takagi, 2021), far from existing ground-based TGF detectors. On the other hand, it is also possible that not all strokes satisfying the ECS criteria are associated with downward TGFs. We suggest that the likelihood of TGF production may be related to the peak current of ECSs, with weaker peak currents corresponding to a lower possibility of TGF occurrence. Further coordinated radio and TGF observations are needed to clarify the most essential common characteristics of ECSs that are associated with downward TGFs.

Data Availability Statement

Data of ECSs and downward TGFs analyzed in the paper can be found at https://doi.org/10.5281/zenodo.13708736 (Wu, 2024).

Acknowledgments

This study was supported by the Ministry of Education, Culture, Sports, Science, and Technology of Japan (Grants 24H00269 and 24H00257) and National Science Foundation (Grant AGS-2235299).

References

Abbasi, R., Abe, M., Abu-Zayyad, T., Allen, M., Anderson, R., Azuma, R., et al. (2017). The bursts of high energy events observed by the telescope array surface detector. *Physics Letters A*, *381*(32), 2565–2572. https://doi.org/10.1016/j.physleta.2017.06.022

Abbasi, R. U., Abu-Zayyad, T., Allen, M., Barcikowski, E., Belz, J. W., Bergman, D. R., et al. (2018). Gamma ray showers observed at ground level in coincidence with downward lightning leaders. *Journal of Geophysical Research: Atmospheres*, *123*(13), 6864–6879. https://doi.org/10.1029/2017jd027931

Albrechtsen, K. H., Østgaard, N., Berge, N., & Gjesteland, T. (2019). Observationally weak TGFS in the RHESSI data. *Journal of Geophysical Research: Atmospheres*, *124*(1), 287–298. https://doi.org/10.1029/2018jd029272

Belz, J. W., Krehbiel, P. R., Remington, J., Stanley, M. A., Abbasi, R. U., LeVon, R., et al. (2020). Observations of the origin of downward terrestrial gamma-ray flashes. *Journal of Geophysical Research: Atmospheres*, *125*(23). https://doi.org/10.1029/2019jd031940

Bowers, G. S., Smith, D. M., Martinez-McKinney, G. F., Kamogawa, M., Cummer, S. A., Dwyer, J. R., et al. (2017). Gamma ray signatures of neutrons from a terrestrial gamma ray flash. *Geophysical Research Letters*, *44*(19). https://doi.org/10.1002/2017gl075071

Cummer, S. A., Lyu, F., Briggs, M. S., Fitzpatrick, G., Roberts, O. J., & Dwyer, J. R. (2015). Lightning leader altitude progression in terrestrial gamma-ray flashes. *Geophysical Research Letters*, *42*(18), 7792–7798. https://doi.org/10.1002/2015gl065228

Cummer, S. A., Zhai, Y., Hu, W., Smith, D. M., Lopez, L. I., & Stanley, M. A. (2005). Measurements and implications of the relationship between lightning and terrestrial gamma ray flashes. *Geophysical Research Letters*, *32*(8). https://doi.org/10.1029/2005gl022778

Dwyer, J. R. (2012). The relativistic feedback discharge model of terrestrial gamma ray flashes. *Journal of Geophysical Research*, *117*(A2). https://doi.org/10.1029/2011ja017160

Dwyer, J. R., Rassoul, H. K., Al-Dayeh, M., Caraway, L., Wright, B., Chrest, A., et al. (2004). A ground level gamma-ray burst observed in association with rocket-triggered lightning. *Geophysical Research Letters*, *31*(5). https://doi.org/10.1029/2003gl018771

Dwyer, J. R., Schaal, M. M., Cramer, E., Arabshahi, S., Liu, N., Rassoul, H. K., et al. (2012). Observation of a gamma-ray flash at ground level in association with a cloud-to-ground lightning return stroke. *Journal of Geophysical Research*, *117*(A10). https://doi.org/10.1029/2012ja017810

Hare, B. M., Uman, M. A., Dwyer, J. R., Jordan, D. M., Biggerstaff, M. I., Caicedo, J. A., et al. (2016). Ground-level observation of a terrestrial gamma ray flash initiated by a triggered lightning. *Journal of Geophysical Research: Atmospheres*, *121*(11), 6511–6533. https://doi.org/10.1002/2015jd024426

Hisadomi, S., Nakazawa, K., Wada, Y., Tsuji, Y., Enoto, T., Shinoda, T., et al. (2021). Multiple gamma-ray glows and a downward TGF observed from nearby thunderclouds. *Journal of Geophysical Research: Atmospheres*, *126*(18). https://doi.org/10.1029/2021jd034543

Ishii, M., & Saito, M. (2009). Lightning electric field characteristics associated with transmission-line faults in winter. *IEEE Transactions on Electromagnetic Compatibility*, *51*(3), 459–465. https://doi.org/10.1109/temc.2009.2025496

Jensen, D., Smith, D. M., Shao, X.-M., & Lapierre, J. (2024). A terrestrial gamma-ray flash observed in coincidence with 3d lightning mapping. AGU24.

Liu, N., & Dwyer, J. R. (2013). Modeling terrestrial gamma ray flashes produced by relativistic feedback discharges. *Journal of Geophysical Research: Space Physics*, *118*(5), 2359–2376. https://doi.org/10.1002/jgra.50232

Lu, G., Blakeslee, R. J., Li, J., Smith, D. M., Shao, X.-M., McCaul, E. W., et al. (2010). Lightning mapping observation of a terrestrial gamma-ray flash. *Geophysical Research Letters*, *37*(11). https://doi.org/10.1029/2010gl043494

Lyu, F., Cummer, S. A., Briggs, M., Marisaldi, M., Blakeslee, R. J., Bruning, E., et al. (2016). Ground detection of terrestrial gamma ray flashes from distant radio signals. *Geophysical Research Letters*, *43*(16), 8728–8734. https://doi.org/10.1002/2016gl070154

Lyu, F., Cummer, S. A., Briggs, M., Smith, D. M., Mailyan, B., & Lesage, S. (2021). Terrestrial gamma-ray flashes can be detected with radio measurements of energetic in-cloud pulses during thunderstorms. *Geophysical Research Letters*, *48*(11). https://doi.org/10.1029/2021gl093627

Lyu, F., Cummer, S. A., & McTague, L. (2015). Insights into high peak current in-cloud lightning events during thunderstorms. *Geophysical Research Letters*, *42*(16), 6836–6843. https://doi.org/10.1002/2015gl065047

Marisaldi, M., Fuschino, F., Labanti, C., Galli, M., Longo, F., Del Monte, E., et al. (2010). Detection of terrestrial gamma ray flashes up to 40 mev by the Agile satellite. *Journal of Geophysical Research*, *115*(A3). https://doi.org/10.1029/2009ja014502

Ortberg, J., Smith, D. M., Kamogawa, M., Dwyer, J., Bowers, G., Chaffin, J., et al. (2024). Two laterally distant TGFS from negative cloud-to-ground strokes in Uchinada, Japan. *Journal of Geophysical Research: Atmospheres*, *129*(2). https://doi.org/10.1029/2023jd039020

Shao, X., Hamlin, T., & Smith, D. M. (2010). A closer examination of terrestrial gamma-ray flash-related lightning processes. *Journal of Geophysical Research*, *115*(A6). https://doi.org/10.1029/2009ja014835

Shi, D., Wang, D., Wu, T., & Takagi, N. (2019). Correlation between the first return stroke of negative CG lightning and its preceding discharge processes. *Journal of Geophysical Research: Atmospheres*, *124*(15), 8501–8510. https://doi.org/10.1029/2019jd030593

Smith, D. M., Bowers, G. S., Kamogawa, M., Wang, D., Ushio, T., Ortberg, J., et al. (2018). Characterizing upward lightning with and without a terrestrial gamma ray flash. *Journal of Geophysical Research: Atmospheres*, *123*(20). https://doi.org/10.1029/2018jd029105

Smith, D. M., Buzbee, P., Kelley, N. A., Infanger, A., Holzworth, R. H., & Dwyer, J. R. (2016). The rarity of terrestrial gamma-ray flashes: 2. RHESSI stacking analysis. *Journal of Geophysical Research: Atmospheres*, *121*(19). https://doi.org/10.1002/2016jd025395

Smith, D. M., Dwyer, J. R., Hazelton, B. J., Grefenstette, B. W., Martinez-McKinney, G. F. M., Zhang, Z. Y., et al. (2011). The rarity of terrestrial gamma-ray flashes: Rare TGFS. *Geophysical Research Letters*, *38*(8). https://doi.org/10.1029/2011gl046875

Stanley, M. A., Shao, X., Smith, D. M., Lopez, L. I., Pongratz, M. B., Harlin, J. D., et al. (2006). A link between terrestrial gamma-ray flashes and intracloud lightning discharges. *Geophysical Research Letters*, *33*(6). https://doi.org/10.1029/2005gl025537

Tilles, J. N., Krehbiel, P. R., Stanley, M. A., Rison, W., Liu, N., Lyu, F., et al. (2020). Radio interferometer observations of an energetic in-cloud pulse reveal large currents generated by relativistic discharges. *Journal of Geophysical Research: Atmospheres*, *125*(20). https://doi.org/10.1029/2020jd032603

Tran, M., Rakov, V., Mallick, S., Dwyer, J., Nag, A., & Heckman, S. (2015). A terrestrial gamma-ray flash recorded at the lightning observatory in Gainesville, Florida. *Journal of Atmospheric and Solar-Terrestrial Physics*, *136*, 86–93. https://doi.org/10.1016/j.jastp.2015.10.010

Tsurumi, M., Enoto, T., Ikkatai, Y., Wu, T., Wang, D., Shinoda, T., et al. (2023). Citizen science observation of a gamma-ray glow associated with the initiation of a lightning flash. *Geophysical Research Letters*, *50*(13). https://doi.org/10.1029/2023gl103612

Wada, Y., Enoto, T., Nakamura, Y., Furuta, Y., Yuasa, T., Nakazawa, K., et al. (2019). Gamma-ray glow preceding downward terrestrial gamma-ray flash. *Communications Physics*, *2*(1), 67. https://doi.org/10.1038/s42005-019-0168-y

Wada, Y., Enoto, T., Nakamura, Y., Morimoto, T., Sato, M., Ushio, T., et al. (2020). High peak-current lightning discharges associated with downward terrestrial gamma-ray flashes. *Journal of Geophysical Research: Atmospheres*, *125*(4). https://doi.org/10.1029/2019jd031730

Wada, Y., Morimoto, T., Nakamura, Y., Wu, T., Enoto, T., Nakazawa, K., et al. (2022). Characteristics of low-frequency pulses associated with downward terrestrial gamma-ray flashes. *Geophysical Research Letters*, *49*(5). https://doi.org/10.1029/2021gl097348

Wada, Y., Wu, T., Wang, D., Enoto, T., Nakazawa, K., Morimoto, T., et al. (2023). Termination of downward-oriented gamma-ray glow by normal-polarity in-cloud discharge activity. *Journal of Geophysical Research: Atmospheres*, *128*(15). https://doi.org/10.1029/2023jd038606

Wu, T. (2024). Energetic compact strokes as the major source of downward terrestrial gamma-ray flashes in winter thunderstorms [Dataset]. *Zenodo*. https://doi.org/10.5281/ZENODO.13708735

Wu, T., Wang, D., Huang, H., & Takagi, N. (2021). The strongest negative lightning strokes in winter thunderstorms in Japan. *Geophysical Research Letters*, *48*(21). https://doi.org/10.1029/2021gl095525

Wu, T., Wang, D., & Takagi, N. (2018). Lightning mapping with an array of fast antennas. *Geophysical Research Letters*, *45*(8), 3698–3705. https://doi.org/10.1002/2018gl077628

Wu, T., Wang, D., & Takagi, N. (2020). Multiple-stroke positive cloud-to-ground lightning observed by the falma in winter thunderstorms in Japan. *Journal of Geophysical Research: Atmospheres*, *125*(20), e2020JD033039. https://doi.org/10.1029/2020JD033039

Wu, T., Wang, D., & Takagi, N. (2021). Compact lightning strokes in winter thunderstorms. *Journal of Geophysical Research: Atmospheres*, *126*(15). https://doi.org/10.1029/2021jd034932

Wu, T., Yoshida, S., Ushio, T., Kawasaki, Z., Takayanagi, Y., & Wang, D. (2014). Large bipolar lightning discharge events in winter thunderstorms in Japan. *Journal of Geophysical Research: Atmospheres*, *119*(2), 555–566. https://doi.org/10.1002/2013jd020369